
Article

Potent antiviral activity against HSV-1 and SARS-CoV-2 by antimicrobial peptoids

Gill Diamond^{1,*}, Natalia Molchanova^{2,7}, Claudine Herlan^{2,3}, John A. Fortkort², Jennifer S. Lin^{2,7}, Erika Figgins¹, Nathan Bopp⁸, Lisa K. Ryan⁴, Donghoon Chung⁵, Robert Scott Adcock⁵, Michael Sherman⁶, and Annelise E. Barron^{2,7,*}

¹ Department of Oral Immunology and Infectious Diseases, University of Louisville School of Dentistry, Louisville, KY 40202 USA; gill.diamond@louisville.edu; erika.figgins@louisville.edu

² Department of Bioengineering, Stanford University, School of Medicine, Stanford, CA 94305; fortkort@stanford.edu; jlin3@stanford.edu; fortkort@stanford.edu; aebarron@stanford.edu

³ Institute of Organic Chemistry, Karlsruhe Institute of Technology, 76131 Karlsruhe, Germany; claudine.herlan@kit.edu

⁴ Division of Infectious Diseases and Global Medicine, Department of Medicine, University of Florida School of Medicine, Gainesville, FL 32601 USA; lisa.ryan@medicine.ufl.edu

⁵ Department of Microbiology, Center for Predictive Medicine, School of Medicine, University of Louisville, KY 40202; hoon.chung@louisville.edu; scott.adcock@louisville.edu

⁶ Department of Biochemistry and Molecular Biology, Sealy Center for Structural Biology and Molecular Biophysics, University of Texas Medical Branch, Galveston, TX 77555; mbsherma@utmb.edu

⁷ Molecular Foundry, Lawrence Berkeley National Laboratory, Berkeley, CA 94720, USA; molchanova.tasha@gmail.com

⁸ Department of Pathology, University of Texas Medical Branch, Galveston, TX 77555; nebopp@utmb.edu

* Correspondence: aebarron@stanford.edu; gill.diamond@louisville.edu

Abstract: Viral infections, such as those caused by Herpes Simplex Virus-1 (HSV-1) and SARS-CoV-2, affect millions of people each year. However, there are few antiviral drugs that can effectively treat these infections. The standard approach in the development of antiviral drugs involves the identification of a unique viral target, followed by the design of an agent that addresses that target. Antimicrobial peptides (AMPs) represent a novel source of potential antiviral drugs. AMPs have been shown to inactivate numerous different enveloped viruses through the disruption of their viral envelopes. However, the clinical development of AMPs as antimicrobial therapeutics has been hampered by a number of factors, especially their structure as peptides. We have examined the antiviral potential of peptoid mimics of AMPs (sequence-specific *N*-substituted glycine oligomers). These peptoids have the distinct advantage of being insensitive to proteases, and also exhibit increased bioavailability and stability. Our results demonstrate that several peptoids exhibit potent *in vitro* antiviral activity against both HSV-1 and SARS-CoV-2 when incubated prior to infection. Visualization by cryo-EM shows viral envelope disruption similar to what has been observed with AMP activity against other viruses. This suggests a common or biomimetic mechanism, possibly due to the differences between the phospholipid head group makeup of viral envelopes and host cell membranes. Furthermore, we observed no cytotoxicity against primary cultures of oral epithelial cells, thus underscoring the potential of this class of molecules as safe and effective broad-spectrum antiviral agents.

Keywords: Antivirals; peptoids, LL-37, air-liquid interface; cytotoxicity; membrane disruption; COVID-19; HSV-1; SARS-CoV-2

1. Introduction

Herpes simplex virus type-1 (HSV-1) infections cause recurrent oral lesions in the developed world, and are also the primary cause of infectious blindness and genital infections in developed countries. These infections can be life-threatening in immunocompromised individuals [1]. Furthermore, there is recent evidence that HSV-1 infections are associated with the pathogenesis of Alzheimer's disease [2]. The HSV-1 virus is transmitted readily through oral secretions. It is estimated that 40-80% of the population is infected with this agent, depending on age and socioeconomic status [3]. The primary class of antiviral therapeutics for this pathogen are nucleoside analogues, such as acyclovir. While acyclovir treatment can reduce the symptoms and shorten the duration of the lesions, it is only effective when given orally, and only reduces the frequency of lesions by approximately 50% [4]. In addition, there is evidence of the development of resistance to this class of antivirals, especially in immunocompromised individuals [5]. Thus, the development of new, effective antiviral agents, which can be used topically to inactivate the virus, is a necessity.

The innate immune system is one of the primary mechanisms for recognizing and eliminating pathogens from mucosal surfaces (reviewed in [6]). Antimicrobial peptides (AMPs) represent an important component of this defense. AMPs are ubiquitous, integral components of innate immunity across phyla, and are promising leads for new antiviral therapies [7] through a number of possible mechanisms. For example, we have recently shown that the human cathelicidin AMP, LL-37, is virucidal for Kaposi's Sarcoma-associated Herpes Virus (KSHV), through a mechanism by which the cationic peptide disrupts the viral envelope [8].

While many AMPs are potent and selective antibiotics, the typically poor bioavailability of peptides limits their clinical use primarily to topical applications. As a result, only a few AMPs are currently being targeted for systemic delivery [9, 10]. Additionally, despite advances in chemical synthesis, manufacturing costs of peptides are still higher in comparison to small-molecule drugs [9, 11]. Moreover, while it is possible to improve the protease resistance of AMPs (while maintaining their activity) by designing them with all D-amino acids, this approach significantly increases the cost of peptide synthesis [12, 13].

The challenges of using AMPs as therapeutics has spurred the development of non-natural peptidomimetics such as 'peptoids', which are sequence-specific N-substituted glycine oligomers [14, 15]. Peptoids are isomerically related to peptides in that their side chains are appended to the backbone amide nitrogens rather than to backbone α -carbons. As a result, peptoids are not proteolyzed by proteases that may be present in the host environment. Furthermore, compared to their peptide counterparts, peptoids have improved biostability and bioavailability, and reduced immunogenicity [16, 17]. Peptoid monomer sequences can be designed to form highly stable, amphipathic helices that do not denature. In particular, unlike the helices of peptides which are stabilized by labile hydrogen bonds, the helices of peptoids are stabilized mostly by steric, van der Waal's and other electronic forces [18-20].

Another major advantage of peptoids is that they can be readily synthesized on a peptide synthesizer (typically using a commercially available RinkTM Amide resin), and can be cleaved by trifluoroacetic

Citation: Lastname, F.; Lastname, F.;
Lastname, F. Title. *Pharmaceuticals*
2021, 14, x.
<https://doi.org/10.3390/xxxxx>

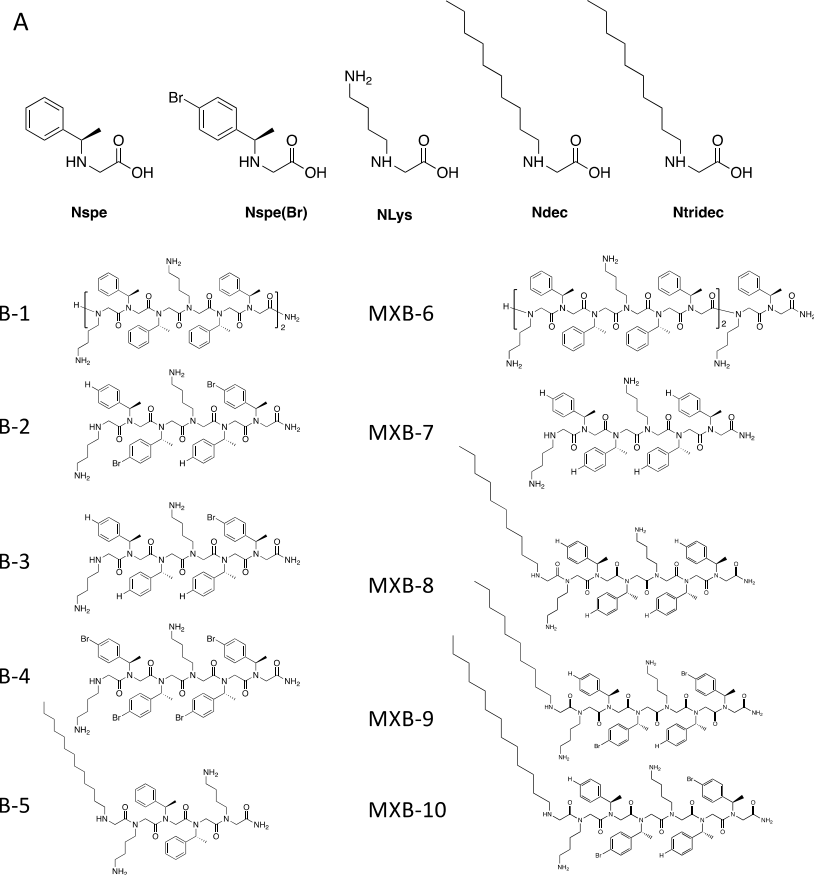
acid and purified by HPLC. The stepwise “sub-monomer” procedure of adding peptoid repeat units is simpler and less costly than that the corresponding synthesis of peptides [21]. This procedure can be programmed into an automated peptide synthesizer, allowing easy introduction of a variety of side chains that can mimic the structures of most of the 20 natural amino acids [22]. Antimicrobial peptoids have been shown to be analogous to AMPs in terms of their efficacy and structure-activity relationships, thus, suggesting that the two classes of antimicrobial compounds operate via analogous mechanisms [14, 23-25]. Furthermore, they are generally non-immunogenic, requiring the attachment of a carrier protein to produce an antibody response [26]. Thus, antimicrobial peptoids have significant potential to be developed as a novel class of biostable, peptidomimetic drugs with advantageous properties.

Based on the results demonstrating the inactivation of enveloped viruses with AMPs through a membrane-disruption mechanism, we hypothesized that antimicrobial peptoids would inactivate an enveloped virus such as HSV-1. In addition, since the recently emerged virus, SARS-CoV-2 (the etiologic agent of COVID-19), is similarly enveloped, we further hypothesized that these peptoids would exhibit similar activity against this devastating virus.

2. Results

We tested the 10 peptoids shown in Figure 1B (as well as the natural human host defense peptide LL-37) for activity against HSV-1. This was accomplished by incubating the virus with the peptoid at 20 $\mu\text{g/ml}$ for 2 hr at 37°C, prior to using the incubated virus to infect cultures of OKF6/TERT-1 cells. An initial screening of the peptoids (Figure 2A) showed wide variability in activity, with MXB-10 exhibiting no activity. We chose five peptoids to study further. The results in Figure 2B show a dose-dependence with strong activity at 20 $\mu\text{g/ml}$ for three of them. MXB-4 and MXB-5 showed a time-dependent inactivation of HSV-1, with activity seen as early as 30 minutes. MXB-9 exhibited the most potent activity, with complete inhibition of the virus after as little as 30 minutes (Figure 2C). Since the virus strain expressed Green Fluorescent Protein (GFP), we could observe the fluorescence at 24 hours post-infection. The control (medium) treated virus exhibited strong fluorescence, while the cultures infected with the virus treated with MXB-5 showed very weak fluorescence in a small number of fluorescent cells. We were required to increase the exposure significantly in order to observe any fluorescence in the peptoid-treated cultures, which led to a bright background (Figure 2D).

Figure 1. Structure of peptoids. A. Structure of



monomers. **B.** Structures of peptoids used in this study.

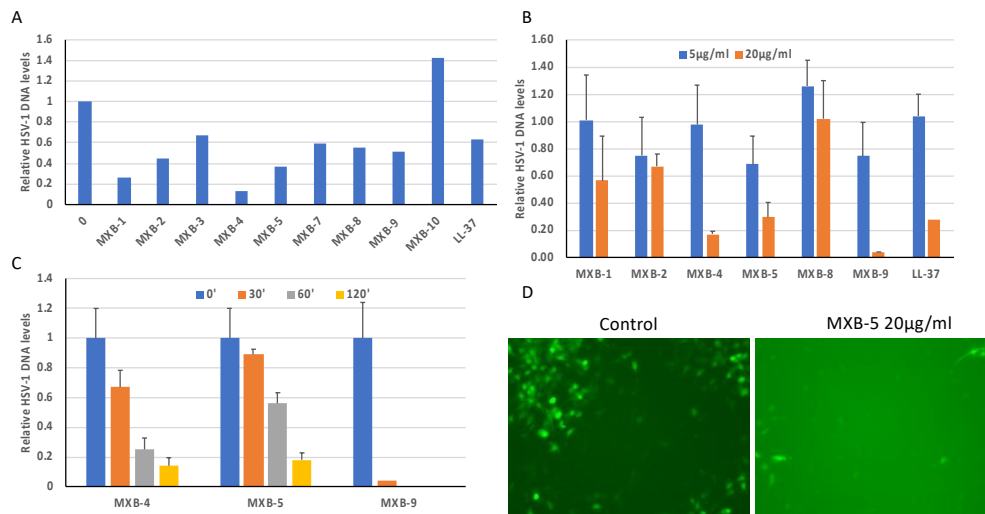
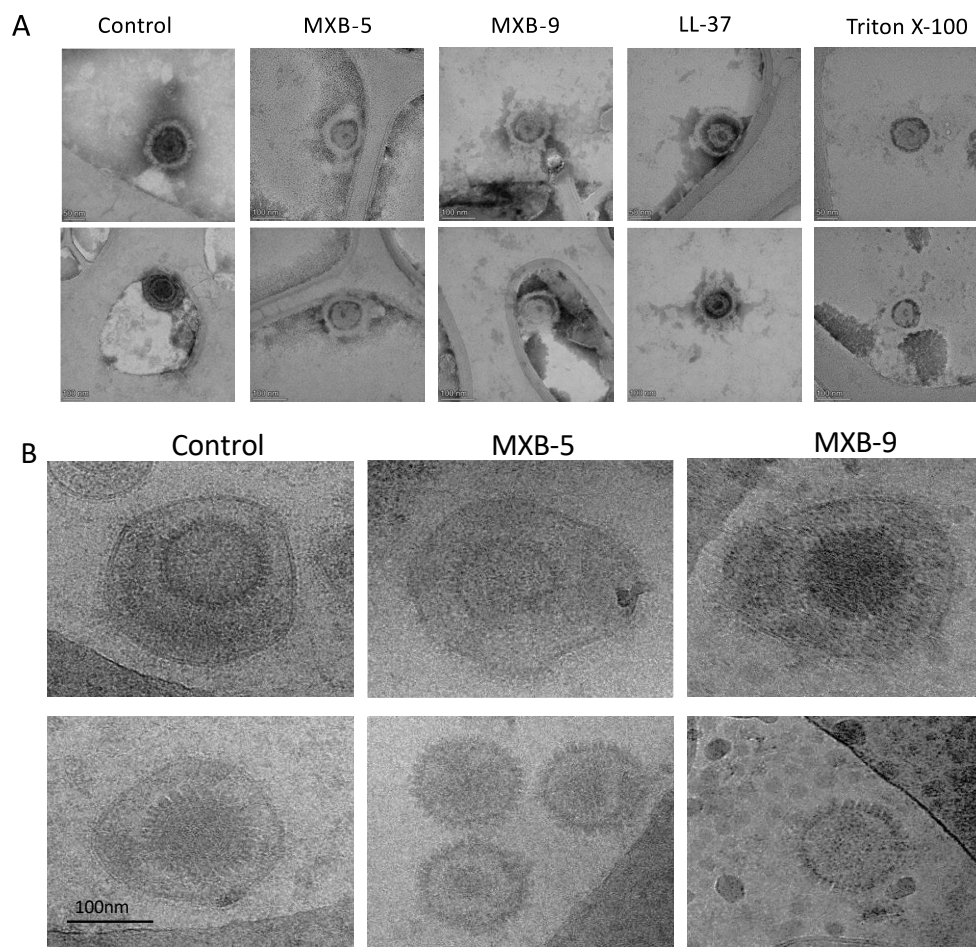


Figure 2. Activity of peptoids and of LL-37 against HSV-1. A. Screening of peptoids against HSV, with comparison to the antiviral activity of LL-37, which is known to be active against HSV-1. The virus was treated with peptoids at 20 µg/ml for 2 hr at 37°C, followed by infection of OKF6/TERT1 cells for 24 hours. Total DNA was isolated and HSV-1 DNA was quantified by QPCR relative to β-actin. B. Activity of peptoids MXB-4, MXB-5 and MXB-9 at 5 µg/ml and 20 µg/ml for 2 hr. C. Time course of MXB-4, MXB-5 and MXB-9 activity. D. Fluorescence imaging of HSV-1

infection 24 hr. after treatment with either control (media) or MXB-5 (20 $\mu\text{g}/\text{ml}$ for 2hr). Results shown are representative of at least two independent experiments.

Our previous results demonstrated that LL-37 disrupted the membrane of KSHV [8]. Thus, we hypothesized that these peptoids, which are simple structural mimics of similar types of peptides, would act through a similar biophysical mechanism. To examine this, we treated HSV-1 with peptoids, followed by electron microscope imaging. Using negative staining EM (Figure 3A) we observed disruption of the membrane in all treated samples, compared with virus treated with PBS alone. Since negative staining procedure could potentially cause modification of the virus owing to chemical treatment of the sample by heavy metal (tungsten) salt, we decided to verify results by using cryo-EM without chemical fixation or negative staining. Both techniques lead to the same conclusion.

Selected examples of cryo-EM images are shown in Figure 3B. The images show clearly resolved viral envelope in the control panels. In the treated samples, there are images showing both partially disrupted envelopes, as well as numerous capsids without envelopes, suggesting a total disruption of the membrane. Quantification of the images (Figure 3C) show that while a small number (21%) of unenveloped capsids are observed in the untreated controls, we see a large increase in both unenveloped capsids (bottom panels, MXB-5 and MXB-9) and disrupted envelopes (top panels). These results are similar to what we observed with treatment of KSHV with LL-37 [8].



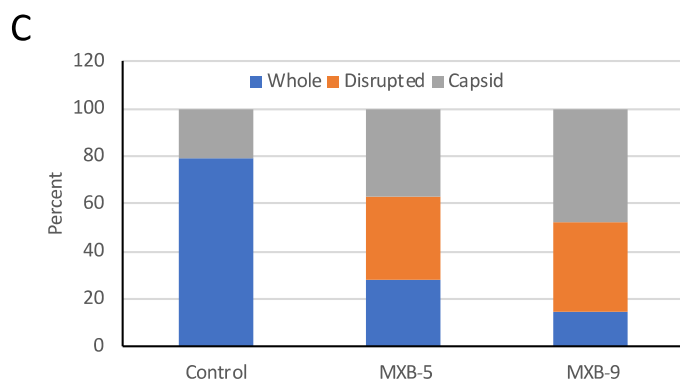


Figure 3: Transmission electron microscope imaging of peptoid-treated HSV-1. Virus was treated for 2 hours at 37°C followed by preparation for EM imaging as described in Materials and Methods. **A.** Negative stained EM. **B.** Cryo-EM. Visible in the control samples are the viral envelope and intact capsid (both panels). In the samples treated with the peptoids we observe both disrupted envelopes (top panels) and naked capsids (bottom panels). **C.** Quantification of whole virus, disrupted envelopes and naked capsids from cryo-EM images.

To determine whether the peptoids would exhibit similar activity against other enveloped viruses, we tested the inhibitory activity of MXB-4 and MXB-9 against SARS-CoV-2. When incubated with virus for 1 hour at 37°C at increasing concentrations, we observed antiviral activity with approximate IC_{50} values of 20 $\mu\text{g/ml}$ and 7 $\mu\text{g/ml}$, respectively (Figure 4). Thus, these two peptoids are active at similar relative concentrations against both viruses.

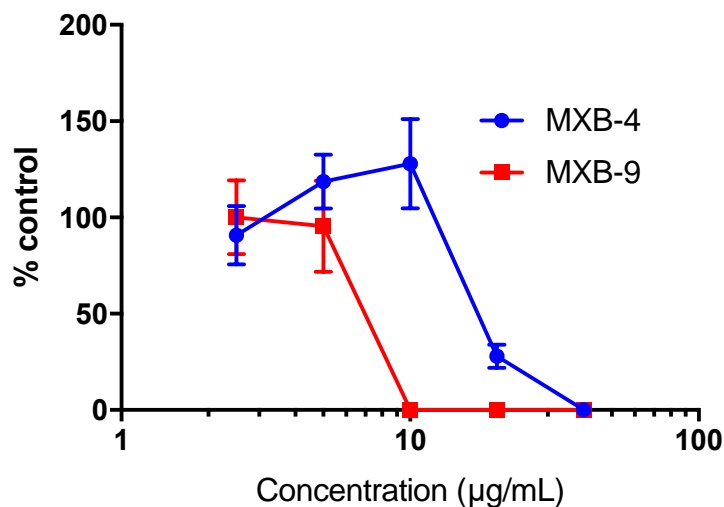


Figure 4: Antiviral activity against SARS-CoV-2. Virus was incubated with peptoids or PBS (control) for 1 hr at 37°C ($n=3$ per condition), prior to infecting Vero E6 cells. After 3 days, total plaques were counted. Data are expressed as percent of control-treated virus. Results shown are representative of two independent replicate experiments.

To determine whether the peptoids acted through a similar membrane-dependent mechanism as with HSV-1, we treated SARS-CoV-2 with the two active peptoids (MXB-4 and MXB-9) followed by visualization by Cryo-EM. While SARS coronaviruses do not exhibit the well-formed hexagonal capsids observed in HSV-1 [27], we observed numerous partially disrupted envelopes as well as what appear to be unenveloped nucleocapsids (Figure 5). We did not observe these structures in the control samples, suggesting that the peptoids are

acting through a similar membrane-disruptive mechanism on both types of virus.

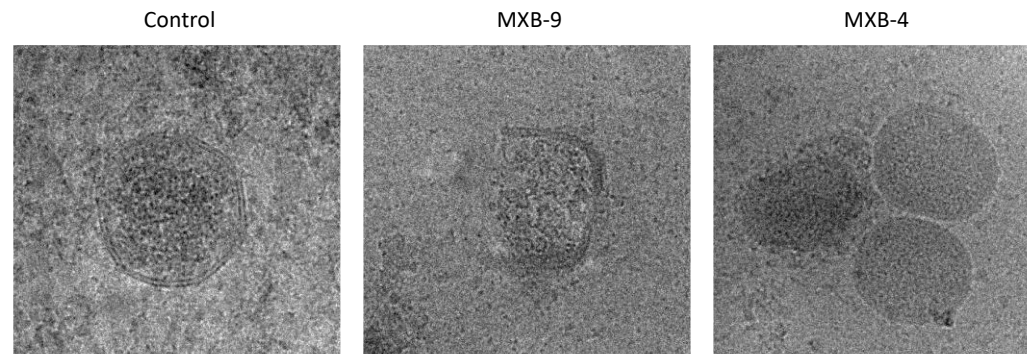


Figure 5. Cryo-EM imaging of peptoid-treated SARS-CoV-2. Virus was treated for 2 hours at 37°C followed by preparation for EM imaging as described in Materials and Methods. Visible are partially disrupted membrane (center) and completely absent membrane (right panel, next to two unaffected virions).

To provide further evidence to support the development of these agents as potential therapeutics, we assayed cytotoxicity against cultured cells. To provide the optimal *in vitro* toxicity model, we used 3-dimensional primary cultures of oral epithelial cells (EpiOral, MatTek), grown at an air-liquid interface. The cultures were tested in the presence of increasing concentrations of MXB-4, MXB-5 and MXB-9 for 3 hours, applied to the apical surface. Viability was monitored using the MTT assay. The results in Figure 6 show no observable toxicity at any concentration up to 256 $\mu\text{g}/\text{ml}$. Incubation with 50% ethanol led to 0% viability (not shown).

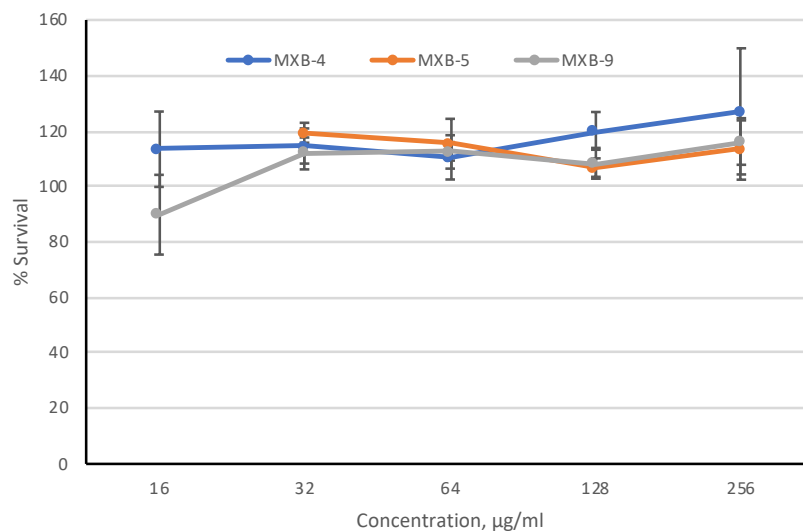


Figure 6. *In vitro* toxicity of peptoids. Peptoids were incubated on the apical surface of cultured EpiAirway cells ($n=3$ wells per concentration) for 3hr. Cell viability was quantified by MTT assay and are shown as mean percent survival \pm SD. Results shown are representative of two independent replicate experiments.

3. Discussion

Herpesvirus infections are common and easily transmissible. However, due to the mechanism of infection and pathogenesis at play,

it has been difficult to design any effective vaccines to prevent herpesvirus infections. Furthermore, other preventive and palliative methods have been challenging to adapt to broad clinical use. Since AMPs such as LL-37 exhibit potent activity against HSV-1 [28], their potential as antiviral preventive or therapeutic agents is significant. However, direct introduction of these peptides has not translated into effective treatments, due to high cost, molecular instability, and unknown pharmacokinetics, among other problems [29, 30]. Here, we have demonstrated the potential use of a novel AMP mimetic structure which, based on its mechanism of action, not only inactivates HSV-1, but can be used against other, more severe enveloped viral pathogens such as SARS-CoV-2.

Conventional development of antiviral therapeutics usually is based on designing drugs that target enzymes or other targets specific to each virus. On rare occasions, drugs such as Remdesivir, which was originally designed to treat Ebola virus infections by targeting the RNA-dependent RNA polymerase of the virus, can have some efficacy in COVID-19 [31]. However, in general, this means that new therapeutic agents must be developed for each virus. The advantage of AMPs and antimicrobial peptoids is that they often target membranes, regardless of microbial species. In many cases, AMPs have been shown to disrupt the viral envelope, although other non-membrane dependent mechanisms have also been observed [7]. Confirming the results of Gordon et al. [28], and in contrast to the results shown by Roy et al. [32], we observe direct inactivation of HSV-1 by LL-37 outside of the cell. This inactivation is presumably due to the damage to the viral envelope we observed by EM, which would prevent binding and infection. This is in contrast to the small antiviral molecule, LJ001. This therapeutic intercalates into the viral envelope, thus interfering in membrane fusion, without causing envelope disruption [33]. Thus, we hypothesized that antimicrobial peptoids would similarly inactivate enveloped viruses. Our results clearly show inactivation of HSV-1, with variable activity between the peptoids.

Comparing the structures of the ten peptoids on our new library with regard to antiviral activity, halogenation seems to be beneficial as every active compound (except MXB-5) includes at least two *N*spe(p-Br) submonomers. Interestingly, shortening of the peptoid oligomers seems to be an issue as well. MXB-5 is the only derivative that is not characterized by at least two helix turns, but shows strong activity despite its lack of halogen substituents. HSV-1 inhibition appears strongly structure-dependent, as slight changes result in structure give rise to significantly different activities. For example, while MXB-9 exhibits potent antiviral activity, its structural analog MXB-10 has no effects on viral propagation.

Lack of cytotoxicity for the host cell is important for any therapeutic. Since HSV-1 generally affects oral epithelial tissues, we tested the active peptoids on well-differentiated 3D cultures of oral epithelium. The drugs were applied to the apical surface, and showed no cytotoxic effects after a 3-hour exposure. This is in line with results routinely obtained with AMPs such as LL-37, which only exhibits cytotoxic effects on host cells at high concentrations [32].

This leads to a very interesting question regarding the mechanism. Our results strongly suggest that, like known AMP activity against bacteria and fungi, the peptoids target and disrupt pathogenic membranes.

For bacteria and fungi, the difference between the microbial membrane and the host cell membrane is striking. Microbial phospholipid bilayers have predominantly anionic headgroups on the outer leaflet, in contrast to mammalian cells where the anionic headgroups are mostly on the inner leaflet. This allows for increased binding of cationic peptides, which leads to the formation of pores or other membrane disrupting events (reviewed in [34]). However, viral envelopes are obtained from the host cell, thus suggesting that peptoids or peptides would have a similar propensity for binding to viral membranes as they do to the host cell membrane. Since neither peptoids nor peptides exhibit cytotoxicity at the same concentrations at which they exhibit viral inhibition, this implies either that the makeup of the outer leaflet of the viral envelope differs from that of the host cell membrane, or that some other structural features of the viral envelope are encouraging binding. It is known that the envelopes of many enveloped viruses contain phospholipid head groups that differ from those in the host cell membrane, including that of HSV-1 [35]. Indeed, they often contain increased levels of phosphatidylserine, a negatively charged headgroup that is usually found in the inner leaflet of the plasma membrane [36]. This switching allows the virus to appear more like an apoptotic cell in order to increase uptake by host cells. Recently, a cationic AMP was shown to exhibit increased binding to a number of enveloped viruses through binding to the PS on the envelopes of these viruses [37].

Other possible features of the viral envelope that could enhance peptoid binding could include the curvature of membrane (which is much stronger in the small viral particle), or an abundance of negatively charged amino acids in the glycoproteins on the surface of the envelope. Due to its much smaller radius, the outer leaflet of the viral particle has an 11% greater surface area than the inner leaflet (as opposed to cells, in which this difference in surface area is only 0.1%) [38]. This feature may enhance interaction with the peptoid. Furthermore, a recent study showed that LL-37 binds to the spike protein of SARS-CoV-2 [39]. This suggests that the initial interaction of the peptoid with this virus is through binding to the spike protein, rather than to the membrane itself. Further research is necessary to understand completely how AMPs and antimicrobial peptoids can distinguish between viral envelopes and host cell membranes. However, regardless of the specific molecular mechanism, our results suggest that peptoids of the type described herein could be developed as broad-spectrum antivirals that could target numerous enveloped viruses, including those which are highly pathogenic.

4. Materials and Methods

4.1 Viruses

HSV-1-GFP was propagated in Vero E6 cells, plaque purified and titered as described [40]. Stocks were aliquoted and maintained at 10^8 pfu/ml in -80°C . Virus was diluted to 10^5 pfu/ml, and incubated with peptoids at 37°C . Samples were removed and added to cultured OKF6/TERT-1 cells at an MOI of 0.1:1 in triplicate, and incubated at 37°C for 24 hours. Cells were lysed and total DNA was isolated using a DNA isolation kit (Qiagen). HSV-1 genomic DNA was quantified by QPCR relative to genomic α -actin DNA. Results were presented as fold change compared to control.

SARS-CoV-2 (strain USA-WA1/2020 isolate; BEI resource cat# NR-52281) was obtained from BEI resources and amplified in Vero E6 cells. Amplified stock virus was stored at -80°C until used. For antiviral activity test, virus was diluted in cell culture media to 2000 pfu/mL and mixed with peptoids 1:1 in volume. The mixture was further incubated at 37°C for one hour and 250 μL of mixture was added to Vero E6 cells grown in 12-well plates. After one hour of incubation, cells were washed once with PBS and overlaid with Avicel overlay media (1% Avicel in DMEM with 10% FBS). Three days later, the overlay media were removed and cells were stained with crystal violet solution (1% crystal violet, 2% paraformaldehyde, 25% Ethanol) for 4 hours. Viral plaques were counted and compared to the mock treated samples. Experiments were performed with three replicates per treatment.

SARS-CoV-2 (strain USA-WA1/2020 isolate) was provided by the World Reference Center for Emerging Viruses and Arboviruses (WRCEVA). Vero76 cells were infected with an MOI of 3 and the infection allowed to progress for 48 hours. Supernatants from infected cells were collected and a primary centrifugation of 10,000xg was performed for 30 minutes. Supernatants from this centrifugation were carefully removed to prevent the disruption of the pelleted debris. Supernatants were then laid upon a 10mL cushion of 20% sucrose and centrifuged for 3 hours at 100,000xg. Supernatants and sucrose were removed following virus pelleting and the virus pellet resuspended in PBS for immediate cryo-EM processing.

Vero E6 cells (ATCC CRL-1586) were obtained from ATCC and cultured in DMEM (HyClone. Cat. SH30243.FS) with 10% FBS. The cells were cultured in a 37°C incubator with 5% CO_2 and passaged every 7 days.

4.2 Cytotoxicity

Normal human bronchial epithelial cells, obtained from MatTek (EpiAirway) were grown at an air-liquid interface at 37°C . Serial dilutions of peptoid were performed in triplicate using 400 μM peptoid stocks resulting in final concentrations between 200 μM and 6.25 μM . Peptoids were applied to the apical surface of cultures in 100 μl for three hours. Cell viability was quantified using the CyQUANT MTT Cell Viability Assay (ThermoFisher), following the manufacturer's instructions Absorbance was read at 540 nm and percent survival was calculated relative to untreated cultures. Ethanol was used as a positive control for cytotoxicity.

4.3 RNA/DNA Isolation

Cells were harvested and homogenized using Qiagen QIAshredder protocol. The obtained lysate was then used to extract RNA and DNA using the Qiagen RNeasy Plus Micro kit. Once RNA was extracted using the manufacturer protocol, DNA was extracted as described [41]. Using the same RNeasy spin columns 50 μL of 8.0 mM NaOH was added directly to membrane. The tubes were then incubated for 10 minutes at 55°C . DNA was eluted by centrifugation for 3 minutes at 5000 x g.

4.4 Quantitative Polymerase Chain Reaction

qPCR was performed on a BIO RAD myCycler using SsoAdvanced Universal SYBR green supermix (Bio-RAD #1725274). Purified HSV1

DNA (1.5 μ l) was used as the template for each reaction mixture. Relative HSV-1 DNA levels were quantified using HSV UL30 (F: AGAGGGACATCCAGGACTTTGT; R: CAGGCGCTTGTTGGTG-TAC), normalized to β -Actin (F: GGA TCA GCA AGC AGG AGT ATG; R: AGA AAG GGT GTA ACG CCA CTA A) in each sample, and the change in expression was determined using the $2^{-\Delta\Delta Ct}$ method compared to control treated samples.

4.5 Rationale for the Design of the Library of Peptoids

Peptoid 1 [H-(NLys-Nspe-Nspe)₄-NH₂], designated here as MXB-1, is a 12-mer with the trimer sequence motif NLys-Nspe-Nspe repeated four times (structures of the monomers are shown in Figure 1A). It is a helical peptoid with broad-spectrum activity against a variety of pathogens [25, 42], including viruses as shown here; it is also active against fungi [43] and bacterial biofilms [44]. Despite these promising features, early *in vitro* studies raised some concerns about the apparent cytotoxicity of Peptoid 1 (notably, however, Peptoid 1 was found to be reasonably well tolerated when delivered intraperitoneally to treat a bacterial infection [25]). We undertook the development of novel analogs of Peptoid 1 that could exhibit reduced cytotoxicity, without compromising the broad-spectrum antimicrobial characteristics of the compound.

After studying more than 120 peptoid sequence variants, a number of unique peptoids were identified that exhibited potent, broad-spectrum antibacterial *in vitro* activity. Like the human antibacterial peptide LL-37 and MXB-1 itself, these peptoids induce a rapid rigidification of bacterial cytoplasm as their biomimetic mechanism of action [45].

This effort led to the development of MXB5 [H-Ntridec-NLys-Nspe-Nspe-NLys-NH₂], a peptoid with a 13-carbon *N*-terminal alkyl modification, that shares some structural similarities with MXB-1 [46]. MXB-5 was found to be highly active against several pathogens as well as against *Pseudomonas aeruginosa* biofilms [44], and was also found to be significantly less cytotoxic to mammalian cells than MXB-1 [47]. In one *in vivo* experiment which has been presented online [48], mice were infected intratracheally with bioluminescent *Pseudomonas aeruginosa*, and were then treated with MXB-5. The peptoid provided a significant reduction in bacterial loads compared to untreated animals, and was also well tolerated in the lungs of the mice. However, MXB-5 was not active against all of the same pathogens that MXB-1 is active against [2].

Given the partial success of MXB-1 and MXB-5, a further library of compounds was developed by hybridizing the key features of these compounds. The activity and potency of these cationic, amphipathic peptoids was found to be affected by their self-assembly into stable, ellipsoidal micelles (unpublished results; and [49]).

The other contribution to this library came in the form of halogenated peptoids, which were explored by Molchanova et al. [49]. They synthesized a library of 36 halogenated analogs of MXB-1. These peptoids contained fluorine, chlorine, bromine and iodine atoms, and varied by length and by the level of halogen substitution in position 4 of the phenyl rings. Compared to an inactive peptoid hexamer comprising half of Peptoid 1 / MXB-1 (NLysNspeNspeNLysNspeNspe), some of these compounds exhibited improved antimicrobial activity.

Molchanova et al. found that short (6mer), brominated analogues of Peptoid 1 not only exhibited reduced cytotoxicity, but relative

to non-brominated compounds, displayed up to a 32-fold increase in activity against *S. aureus* and a 16- to 64-fold increase in activity against *E. coli* and *P. aeruginosa*. They ascribed these results to the relatively increased hydrophobicity and self-assembly properties of the compounds. In particular, they obtained small angle X-ray scattering (SAXS) data which demonstrated how the self-assembled structures are dependent on the size of the halogen, the degree of halogen substitution and the length of the peptoid, and they correlated these features to the activity of the resulting peptoid. Thus, the creation of the peptoid library tested in this study hybridized the molecular features of three different peptoid motifs: (1) inclusion of the N_{Lys}N_{spe}N_{spe} trimer sequence motif; (2) N-terminal alkylation with either a C10 or C13 chain; (3) inclusion of para-brominated (at position 4 in the phenyl ring) N_{spe} monomers. Within a library comprising these attributes, we identified numerous active antiviral peptoids.

4.6 General synthesis of peptoids

Peptoids were synthesized manually in accordance with the submonomer method [21]. All reaction steps were performed in fritted 10 mL syringes under smooth mixing on a VWR® Tube Rocker at 21 °C. Rink amide MBHA resin (Protein Technologies Inc., 0.64 mmol/g) was used as a solid support. Acetylation steps were carried out for 30 min, substitution for 1 h. Substitution with alkylamines was performed overnight. Acetylation using bromoacetic acid and substitution by various amines were alternated until the desired chain length was achieved. The single oligomers were cleaved and deprotected simultaneously using a cocktail of trifluoroacetic acid/triisopropylsilane/water (95:2.5:2.5 (v/v)) for 30 min. After purification, exchange of the counterion was carried out using a 10 mM solution of aqueous HCl. Lyophilization yielded the desired compound. Purity was determined to exceed 95%.

4.7 Peptoid purification

Starting materials and solvents were purchased from commercial suppliers (Acros Organics, Alfa Aesar, Chem-Impex Intl. Inc., CNH Technologies, Merck, OmniSolv, Protein Technologies, Sigma-Aldrich, TCI, and VWR) and used without further purification. Water was filtered through a 0.22- μ m Millipore membrane filter.

Product formation and purity were determined by means of analytical UPLC/MS using a Water Acquity UPLC system, equipped with an Acquity Diode Array UV detector and a Waters SQD2 mass spectrometer. As stationary phase, a Waters Acquity UPLC Peptide BEH C18 Column (300 Å pore size, 1.7 μ m particle size, 2.1 mm \times 100 mm) with an Acquity UPLC BEH C18 VanGuard pre-column (1.7 μ m, 2.1 mm \times 5 mm) was employed. For alkylated derivatives, a Waters Acquity UPLC BEH300 C4 column (300 Å pore size, 1.7 μ m particle size, 2.1 mm \times 100 mm) with an Acquity UPLC BEH300 C4 VanGuard pre-column (1.7 μ m, 2.1 mm \times 5 mm) was used. Elution was performed using an aqueous acetonitrile gradient with 0.1% (v/v) trifluoroacetic acid added (5–95% acetonitrile (v/v) over 6.80 min, flow rate: 0.8 mL/min, column temperature: 60 °C). UPLC chromatograms are available in the supporting information (see Supplementary Figure S1). The mass spectra were collected in ESI⁺ mode.

Purification by means of preparative HPLC was carried out using a Waters Prep150LC system, equipped with a Waters 2489

UV/Visible detector and a Waters Fraction Collector III collector. As stationary phase, a Waters XBridge BEH300 Prep C18 column (5 μm particle size, 19 mm \times 100 mm) with a Waters XBridge Peptide BEH300 C18 guard column (5 μm particle size, 19 mm \times 10 mm) was employed. For alkylated derivatives, a Waters Symmetry300 C4 column (5 μm particle size, 19 mm \times 100 mm) with a Waters Symmetry300 C4 guard column (5 μm particle size, 19 mm \times 10 mm) was used. Elution was performed using an aqueous acetonitrile gradient with 0.1% (v/v) trifluoroacetic acid added (20–60% acetonitrile(v/v) over 30 minutes at a flow rate of 17 mL/min).

4.8 Electron microscopy

4.8.1 Negative staining EM:

HSV-1 (1×10^8 pfu/ml) was incubated with peptoids or control medium for 2 hr. at 37°C. After incubation, the virus was fixed by addition of 2 volumes 4% glutaraldehyde/PBS, and fixed at 4°C for 24 hours. Virus was applied to grids (ultrathin carbon with lacey support film, Ted Pella, Inc.) for 1 minute, followed by staining in 1% phosphotungstic acid for 1 minute. Excess liquid was blotted and grids were allowed to air dry. Images were collected using a Thermo Scientific™ Talos™ F200X at 200 kV accelerating voltage with 50 μm objective aperture inserted to enhance contrast. Images were captured using a 4k \times 4k CMOS camera (Thermo Scientific™ Ceta 16M™).

4.8.2 Cryo-EM:

After incubation of HSV-1 virus with peptoids for 2 hr. at 37°C, samples were vitrified using Leica EM-GP2® plunger (Leica Microsystems) as previously described [50] on carbon holey film (R2x1 Quantifoil®; Micro Tools GmbH, Jena, Germany) grids. Briefly, suspensions of virions were applied to the holey films, blotted with filter paper, and plunged into liquid ethane.

SARS Co-V-2 was incubated with peptoids similar to the HSV-1 (two hours at 37°C) and vitrified also on R2x1 Quantifoil grids using a manual cryo-plunger [51] in a biosafety cabinet. All experiments, including EM imaging were performed in a biosafety level 3 (BSL-3) containment because of the NIH/CDC classification of the virus.

The grids were imaged in a JEOL 2200FS electron microscope (JEOL, Japan). The microscope was operated at 200 keV; we used 20 eV electron energy filter slit for image acquisition. A Fischione Instruments 2550 cryo-transfer side-entry holder (E.A. Fischione Instruments, Inc., PA) was used for data collection. The image were acquired on DE-20 (Direct Electron, San Diego, Ca) camera, used in linear mode with 25 frames/s rate. Total electron dose/image was ~ 25 electrons/ \AA^2 . Image pixel size was 1.5 \AA on the specimen scale.

Supplementary Materials: The following are available online at www.mdpi.com/xxx/s1, Figure S1: LC/MS Traces for peptoids.

Author Contributions: Conceptualization, G.D. and A.B.; methodology, D.C., M.S., L.K.R., E.F.; design of peptoids, A.B., N.M., J.S.L.; synthesis of peptoids, CH; investigation, E.F., R.S.A., N.B.; writing—original draft preparation, G.D., N.M., C.H., A.B.; writing—review and editing, G.D., L.K.R., D.C., J.A.F., N.M., C.H., M.S. All authors have read and agreed to the published version of the manuscript.

Funding: This work was funded by grants from Maxwell Biosciences, Inc., and the U.S. Public Health Services (including an NIH Pioneer Award to Annelise

Barron, grant # 1DP1 OD029517-01). Work at the Molecular Foundry was supported by the Office of Science, Office of Basic Energy Sciences, of the U.S. Department of Energy under Contract No. DE-AC02-05CH11231.

Acknowledgments: The authors thank Jillian Cramer for her invaluable assistance with the TEM. This work was performed in part at the Electron Microscopy Center which belongs to the National Science Foundation NNCI Kentucky Multiscale Manufacturing and Nano Integration Node, supported by ECCS-1542174. We also thank Drs. Håvard Jenssen (Roskilde University) and Stefan Bräse (Karlsruhe Institute of Technology) for their support and mentorship.

Conflicts of Interest: A.B. is a shareholder and member of the Board of Directors of Maxwell Biosciences; G.D., N.M. and J.F. are shareholders and consultants for Maxwell Biosciences. The funders had no role in the design of the study; in the collection, analyses, or interpretation of data; in the writing of the manuscript, or in the decision to publish the results.

References

1. Chayavichitsilp, P., Buckwalter, J.V., Krakowski, A.C., and Friedlander, S.F., Herpes simplex. *Pediatr Rev*, **2009**. 30(4): p. 119-29.
2. Harris, S.A. and Harris, E.A., Molecular Mechanisms for Herpes Simplex Virus Type 1 Pathogenesis in Alzheimer's Disease. *Front Aging Neurosci*, **2018**. 10: p. 48.
3. Arduino, P.G. and Porter, S.R., Herpes Simplex Virus Type 1 infection: overview on relevant clinico-pathological features. *J Oral Pathol Med*, **2008**. 37(2): p. 107-21.
4. Spruance, S.L., Stewart, J.C., Rowe, N.H., McKeough, M.B., Wenerstrom, G., and Freeman, D.J., Treatment of recurrent herpes simplex labialis with oral acyclovir. *J Infect Dis*, **1990**. 161(2): p. 185-90.
5. Piret, J. and Boivin, G., Resistance of herpes simplex viruses to nucleoside analogues: mechanisms, prevalence, and management. *Antimicrob Agents Chemother*, **2011**. 55(2): p. 459-72.
6. Diamond, G., Legarda, D., and Ryan, L.K., The Innate Immune Response of the Respiratory Epithelium. *Immunol. Rev.*, **2000**. 173: p. 27-38.
7. Brice, D.C. and Diamond, G., Antiviral Activities of Human Host Defense Peptides. *Curr Med Chem*, **2020**.
8. Brice, D.C., Toth, Z., and Diamond, G., LL-37 disrupts the Kaposi's sarcoma-associated herpesvirus envelope and inhibits infection in oral epithelial cells. *Antiviral Res*, **2018**. 158: p. 25-33.
9. Dostert, M., Belanger, C.R., and Hancock, R.E.W., Design and Assessment of Anti-Biofilm Peptides: Steps Toward Clinical Application. *J Innate Immun*, **2019**. 11(3): p. 193-204.
10. Mahlapuu, M., Hakansson, J., Ringstad, L., and Bjorn, C., Antimicrobial Peptides: An Emerging Category of Therapeutic Agents. *Front Cell Infect Microbiol*, **2016**. 6: p. 194.
11. Henninot, A., Collins, J.C., and Nuss, J.M., The Current State of Peptide Drug Discovery: Back to the Future? *J Med Chem*, **2018**. 61(4): p. 1382-1414.
12. de la Fuente-Nunez, C., Reffuveille, F., Mansour, S.C., Reckseidler-Zenteno, S.L., Hernandez, D., Brackman, G., Coenye, T., and Hancock, R.E., D-enantiomeric peptides that eradicate wild-type and multidrug-resistant biofilms and protect against lethal *Pseudomonas aeruginosa* infections. *Chem Biol*, **2015**. 22: p. 196-205.
13. Bessalle, R., Kapitkovsky, A., Gorea, A., Shalit, I., and Fridkin, M., All-D-magainin: chirality, antimicrobial activity and proteolytic resistance. *FEBS Lett*, **1990**. 274(1-2): p. 151-5.
14. Mojsoska, B. and Jenssen, H., Peptides and Peptidomimetics for Antimicrobial Drug Design. *Pharmaceuticals (Basel)*, **2015**. 8(3): p. 366-415.
15. Patch, J.A. and Barron, A.E., Mimicry of bioactive peptides via non-natural, sequence-specific peptidomimetic oligomers. *Curr Opin Chem Biol*, **2002**. 6(6): p. 872-7.
16. Gibbons, J.A., Hancock, A.A., Vitt, C.R., Knepper, S., Buckner, S.A., Brune, M.E., Milicic, I., Kerwin, J.F., Jr., Richter, L.S., Taylor, E.W., Spear, K.L., Zuckermann, R.N., Spellmeyer, D.C., Braeckman, R.A., and Moos, W.H., Pharmacologic characterization of CHIR 2279, an N-substituted glycine peptoid with high-affinity binding for alpha 1-adrenoceptors. *J Pharmacol Exp Ther*, **1996**. 277(2): p. 885-99.
17. Miller, S.M., Simon, R.J., Ng, S., Zuckermann, R.N., Kerr, J.M., and Moos, W.H., Comparison of the proteolytic susceptibilities of homologous L-amino acid, D-amino acid, and N-substituted glycine peptoid and peptoid oligomers. *Drug Dev. Res.*, **1995**. 35: p. 20-32.
18. Sanborn, T.J., Wu, C.W., Zuckermann, R.N., and Barron, A.E., Extreme stability of helices formed by water-soluble poly-N-substituted glycines (polypeptoids) with alpha-chiral side chains. *Biopolymers*, **2002**. 63(1): p. 12-20.

19. Wu, C.W., Sanborn, T.J., Zuckermann, R.N., and Barron, A.E., Peptoid oligomers with alpha-chiral, aromatic side chains: effects of chain length on secondary structure. *J Am Chem Soc*, **2001**. 123(13): p. 2958-63.
20. Kirshenbaum, K., Barron, A.E., Goldsmith, R.A., Armand, P., Bradley, E.K., Truong, K.T., Dill, K.A., Cohen, F.E., and Zuckermann, R.N., Sequence-specific polypeptoids: a diverse family of heteropolymers with stable secondary structure. *Proc Natl Acad Sci U S A*, **1998**. 95(8): p. 4303-8.
21. Zuckermann, R.N., Kerr, J.M., Kent, S.B.H., and Moos, W.H., Efficient method for the preparation of peptoids [oligo(N-substituted glycines)] by submonomer solid-phase synthesis. *J. Am. Chem. Soc.*, **1992**. 114: p. 10646-10647.
22. Czyzewski, A.M. and Barron, A.E., Protein and peptide biomimicry: Gold-mining inspiration from Nature's ingenuity. *AIChE Journal*, **2007**. 54: p. 2-8.
23. Chongsiriwatana, N.P., Patch, J.A., Czyzewski, A.M., Dohm, M.T., Ivankin, A., Gidalevitz, D., Zuckermann, R.N., and Barron, A.E., Peptoids that mimic the structure, function, and mechanism of helical antimicrobial peptides. *Proc Natl Acad Sci U S A*, **2008**. 105(8): p. 2794-9.
24. Chongsiriwatana, N.P., Wetzler, M., and Barron, A.E., Functional synergy between antimicrobial peptoids and peptides against Gram-negative bacteria. *Antimicrob Agents Chemother*, **2011**. 55(11): p. 5399-402.
25. Czyzewski, A.M., Jenssen, H., Fjell, C.D., Waldbrook, M., Chongsiriwatana, N.P., Yuen, E., Hancock, R.E., and Barron, A.E., In Vivo, In Vitro, and In Silico Characterization of Peptoids as Antimicrobial Agents. *PLoS One*, **2016**. 11(2): p. e0135961.
26. Astle, J.M., Udugamasooriya, G., Smallshaw, J.E., and Kodadek, T., A VEGFR2 Antagonist and Other Peptoids Evade Immune Recognition. *Int. J. Pept. Res. Ther.*, **2008**. 14: p. 223-227.
27. Neuman, B.W., Adair, B.D., Yoshioka, C., Quispe, J.D., Orca, G., Kuhn, P., Milligan, R.A., Yeager, M., and Buchmeier, M.J., Supramolecular architecture of severe acute respiratory syndrome coronavirus revealed by electron cryomicroscopy. *J Virol*, **2006**. 80(16): p. 7918-28.
28. Gordon, Y.J., Huang, L.C., Romanowski, E.G., Yates, K.A., Proske, R.J., and McDermott, A.M., Human cathelicidin (LL-37), a multifunctional peptide, is expressed by ocular surface epithelia and has potent antibacterial and antiviral activity. *Curr Eye Res*, **2005**. 30(5): p. 385-94.
29. Eckert, R., Road to clinical efficacy: challenges and novel strategies for antimicrobial peptide development. *Future Microbiol*, **2011**. 6(6): p. 635-51.
30. Marr, A.K., Gooderham, W.J., and Hancock, R.E., Antibacterial peptides for therapeutic use: obstacles and realistic outlook. *Curr Opin Pharmacol*, **2006**. 6(5): p. 468-72.
31. Sternberg, A., McKee, D.L., and Naujokat, C., Novel Drugs Targeting the SARS-CoV-2/COVID-19 Machinery. *Curr Top Med Chem*, **2020**. 20(16): p. 1423-1433.
32. Roy, M., Lebeau, L., Chessa, C., Damour, A., Ladram, A., Oury, B., Boutolleau, D., Bodet, C., and Leveque, N., Comparison of Anti-Viral Activity of Frog Skin Anti-Microbial Peptides Temporin-Sha and [K(3)]SHA to LL-37 and Temporin-Tb against Herpes Simplex Virus Type 1. *Viruses*, **2019**. 11(1).
33. Wolf, M.C., Freiberg, A.N., Zhang, T., Akyol-Ataman, Z., Grock, A., Hong, P.W., Li, J., Watson, N.F., Fang, A.Q., Aguilar, H.C., Porotto, M., Honko, A.N., Damoiseaux, R., Miller, J.P., Woodson, S.E., Chantasirivisal, S., Fontanes, V., Negrete, O.A., Krogstad, P., Dasgupta, A., Moscona, A., Hensley, L.E., Whelan, S.P., Faull, K.F., Holbrook, M.R., Jung, M.E., and Lee, B., A broad-spectrum antiviral targeting entry of enveloped viruses. *Proc Natl Acad Sci U S A*, **2010**. 107(7): p. 3157-62.
34. Nguyen, L.T., Haney, E.F., and Vogel, H.J., The expanding scope of antimicrobial peptide structures and their modes of action. *Trends Biotechnol*, **2011**. 29(9): p. 464-72.
35. van Genderen, I.L., Brandimarti, R., Torrisi, M.R., Campadelli, G., and van Meer, G., The phospholipid composition of extracellular herpes simplex virions differs from that of host cell nuclei. *Virology*, **1994**. 200(2): p. 831-6.
36. Amara, A. and Mercer, J., Viral apoptotic mimicry. *Nat Rev Microbiol*, **2015**. 13(8): p. 461-9.
37. Luteijn, R.D., Praest, P., Thiele, F., Sadasivam, S.M., Singethan, K., Drijfhout, J.W., Bach, C., de Boer, S.M., Lebbink, R.J., Tao, S., Helfer, M., Bach, N.C., Protzer, U., Costa, A.I., Killian, J.A., Drexler, I., and Wiertz, E., A Broad-Spectrum Antiviral Peptide Blocks Infection of Viruses by Binding to Phosphatidyserine in the Viral Envelope. *Cells*, **2020**. 9(9).
38. Stadler, A.M., Kyritsaka, N., Graff, R., and Lehn, J.M., Formation of RACK-and grid-type metallo-supramolecular architectures and generation of molecular motion by reversible uncoiling of helical ligand strands. *Chemistry*, **2006**. 12: p. 4503-22.
39. Roth, A., Lutke, S., Meinberger, D., Hermes, G., Sengle, G., Koch, M., Streichert, T., and Klatt, A.R., LL-37 fights SARS-CoV-2: The Vitamin D-Inducible Peptide LL-37 Inhibits Binding of SARS-CoV-2 Spike Protein to its Cellular Receptor Angiotensin Converting Enzyme 2 In Vitro. *bioRxiv*, **2020**.
40. Ryan, L.K., Dai, J., Yin, Z., Megjugorac, N., Uhlhorn, V., Yim, S., Schwartz, K.D., Abrahams, J.M., Diamond, G., and Fitzgerald-Bocarsly, P., Modulation of human {beta}-defensin-1 (hBD-1) in

-
- plasmacytoid dendritic cells (PDC), monocytes, and epithelial cells by influenza virus, Herpes simplex virus, and Sendai virus and its possible role in innate immunity. *J Leukoc Biol*, **2011**. *90*: p. 343-56.
41. Martins, W.K., A useful procedure to isolate simultaneously DNA and RNA from a single tumor sample. *Protocol Exchange*, **2009**.
42. Patch, J.A. and Barron, A.E., Helical peptoid mimics of magainin-2 amide. *J Am Chem Soc*, **2003**. *125*(40): p. 12092-3.
43. Uchida, M., McDermott, G., Wetzler, M., Le Gros, M.A., Myllys, M., Knoechel, C., Barron, A.E., and Larabell, C.A., Soft X-ray tomography of phenotypic switching and the cellular response to antifungal peptoids in *Candida albicans*. *Proc Natl Acad Sci U S A*, **2009**. *106*(46): p. 19375-80.
44. Kapoor, R., Wadman, M.W., Dohm, M.T., Czyzewski, A.M., Spormann, A.M., and Barron, A.E., Antimicrobial peptoids are effective against *Pseudomonas aeruginosa* biofilms. *Antimicrob Agents Chemother*, **2011**. *55*(6): p. 3054-7.
45. Chongsiriwatana, N.P., Lin, J.S., Kapoor, R., Wetzler, M., Rea, J.A.C., Didwania, M.K., Contag, C.H., and Barron, A.E., Intracellular biomass flocculation as a key mechanism of rapid bacterial killing by cationic, amphipathic antimicrobial peptides and peptoids. *Sci Rep*, **2017**. *7*(1): p. 16718.
46. Chongsiriwatana, N.P., Miller, T.M., Wetzler, M., Vakulenko, S., Karlsson, A.J., Palecek, S.P., Mobashery, S., and Barron, A.E., Short alkylated peptoid mimics of antimicrobial lipopeptides. *Antimicrob Agents Chemother*, **2011**. *55*(1): p. 417-20.
47. Kapoor, R., Eimerman, P.R., Hardy, J.W., Cirillo, J.D., Contag, C.H., and Barron, A.E., Efficacy of antimicrobial peptoids against *Mycobacterium tuberculosis*. *Antimicrob Agents Chemother*, **2011**. *55*(6): p. 3058-62.
48. Barron, A.E., *Biomimetic Drugs: In vitro, In vivo And Mechanistic Studies of 5-12mer Antimicrobial & Antiviral Peptoids to Treat Respiratory Infections at the Airway Interface*, in *Virtual AIChE Annual Meeting*. 2020.
49. Molchanova, N., Nielsen, J., Sørensen, K., Prabhala, B., Hansen, P., Lund, R., Barron, A., and Jensen, H., Halogenation as a tool to tune antimicrobial activity of peptoids. *Scientific Reports*, **2020**. *10*.
50. Sherman, M.B., Guenther, R., Reade, R., Rochon, D., Sit, T., and Smith, T.J., Near-Atomic-Resolution Cryo-Electron Microscopy Structures of Cucumber Leaf Spot Virus and Red Clover Necrotic Mosaic Virus: Evolutionary Divergence at the Icosahedral Three-Fold Axes. *J Virol*, **2020**. *94*(2).
51. Sherman, M.B. and Weaver, S.C., Structure of the recombinant alphavirus Western equine encephalitis virus revealed by cryoelectron microscopy. *J Virol*, **2010**. *84*(19): p. 9775-82.